DOI: 10.1002/ejoc.200900197

Karplus-Type Dependence of Vicinal ^{119}Sn-^{13}C and ^{119}Sn-^{1}H Spin-Spin Couplings in Organotin(IV) Derivatives: A DFT Study

Girolamo Casella,[a] Francesco Ferrante,[b] and Giacomo Saielli*[c]

Keywords: Relativistic effects / Density functional calculations / NMR spectroscopy / Tin

The empirical Karplus-type dependence of $^{3}J(^{119}Sn,^{13}C)$ and $^{3}J(^{119}Sn,^{1}H)$ couplings in organotin(IV) derivatives has been computationally validated by DFT methods both at the non-relativistic and scalar ZORA relativistic level. A preliminary calibration of the computational protocols, by comparing experimental and calculated couplings for a set of suitable rigid molecules, revealed their high predictive power: in particular, relativistic results for $^{3}J(^{119}Sn,^{13}C)$ have a mean absolute error of just above 2 Hz, over a range of values up to about 70 Hz. The latter protocol has then been used to study in detail the influence of substituents and multiple paths connecting the coupled nuclei on the vicinal coupling constants. Some conformational issues have been also considered. Significant effects have been observed and theoretical Karplus-type curves for some representative systems have been proposed and discussed. It appears that general equations for vicinal ^{119}Sn-^{1}H and ^{119}Sn-^{13}C couplings cannot be derived, although the shape of the curves is preserved with $|^{3}J(0°)| < |^{3}J(180°)|$ and $^{3}J(90°) \approx 0$ Hz.

Introduction

^{119}Sn, ^{1}H and ^{13}C NMR spectroscopy is a powerful tool in organotin(IV) structural studies both in solution phase and in solid state. The huge amount of literature concerning this topic,[1–4] and the ensuing amount of experimental data, allowed to get empirical correlations between the NMR parameters and the molecular structure around the tin atom.

For organotin(IV) derivatives a correlation between ^{119}Sn chemical shift, $\delta(^{119}Sn)$, and tin coordination number has been ascertained since the early years of ^{119}Sn NMR spectroscopy;[1] these data are often supported by the simultaneous analysis of the $\delta(^{1}H)$ and the $\delta(^{13}C)$ in the case of specific classes of organotin(IV) compounds, e.g., $R_nSn^{IV}X_{4-n}$ (n = 2,3; R = methyl, butyl, phenyl, benzyl).[5–11] However, despite the large $\delta(^{119}Sn)$ chemical shift range of organotin(IV) compounds, ca. 600 ppm ranging from tetra- to hexacoordinate tin, and the various factors influencing the ^{119}Sn chemical shift, e.g., solvent effects, self-association and temperature, the latter may not be sufficient for a full structural characterization.

In this respect, spin-spin coupling constants $^{n}J(^{119}Sn, X)$ (n = 1, 2, 3; X = ^{1}H, ^{2}H, ^{13}C) have proven to be a powerful complementary tool in structural studies. In particular, empirical equations correlating the C–Sn–C angle, θ, with the $^{1}J(^{119}Sn,^{13}C)$ value for $Me_nSn^{IV}X_{4-n}$[12,13] and Bu_nSn^{IV}-X_{4-n}[8,14] (n = 2,3) and the $^{2}J(^{119}Sn, ^{1}H)$ for Me_nSn^{IV}-X_{4-n} (n = 2,3) derivatives have been reported.[12] No explicit equations have been proposed to correlate θ with any $^{n}J(^{119}Sn, X)$ (n = 1, 2; X = ^{1}H, ^{13}C), for triphenyl- and tribenzyltin(IV) derivatives. However structural trends in these compounds could be inferred from the $\delta(^{13}C)$ and the $^{n}J(^{119}Sn,^{13}C)$ (n = 1,2,3,4) couplings of the phenyl and benzyl groups and, only for the tribenzyltin(IV) derivatives, from the $^{2}J(^{119}Sn, ^{1}H)$.[9,11]

$^{3}J(^{119}Sn, X)$ (X = ^{1}H, ^{2}H, ^{13}C) play a very important role in organotin(IV) conformational studies, somehow mirroring the distinctive role that the Karplus dependence of $^{3}J(^{1}H,^{1}H)$ on the dihedral angle holds in structure elucidation of organic molecules. Also in this case some empirical relationships have been reported. Kitching and co-workers, starting from a small set or rigid polycyclic organotin(IV) compounds, proposed a Karplus-type equation which correlates the $^{3}J(^{119}Sn\text{-}C\text{-}C\text{-}^{13}C)$ with the dihedral angle, ϕ;[15,16] they also pointed out that the occurrence of more than one conformer in solution for flexible cyclic systems must be taken into account when structural assignments are inferred from the vicinal coupling constants.[17]

[a] Dipartimento di Chimica Inorganica e Analitica "Stanislao Cannizzaro", Università degli Studi di Palermo,
Viale delle Scienze, Parco D'Orleans II, Ed. 17, 90128 Palermo, Italy
[b] Dipartimento di Chimica Fisica "Filippo Accascina", Università degli Studi di Palermo,
Viale delle Scienze, Parco D'Orleans II, Ed. 17, 90128 Palermo, Italy
[c] Istituto per la Tecnologia delle Membrane del CNR, Sezione di Padova,
via Marzolo 1, 35131 Padova, Italy
Fax: +39-049-8275239
E-mail: giacomo.saielli@unipd.it

Supporting information for this article is available on the WWW under http://dx.doi.org/10.1002/ejoc.200900197.

A similar equation was derived by Quintard and co-workers for $^3J(^{119}Sn\text{-}C\text{-}C\text{-}D)$[18] from which it is possible to obtain the corresponding $^3J(^{119}Sn\text{-}C\text{-}C\text{-}^1H)$ dependence by a simple conversion. Other Karplus-type equations have been proposed for the $^3J(^{119}Sn,^{31}P)$[19] and $^3J(^{119}Sn,^{119}Sn)$ couplings.[20]

Conformational studies of organotin derivatives can greatly benefit from the use of Karplus-type equations: for example, weak tin-donor interactions, mainly of van der Waals nature, rather than true coordination bonds, have been highlighted by applying the above Karplus-type relationships to $^3J(^{119}Sn,^{13}C)$ and $^3J(^{119}Sn,^1H)$ in *gem*-bis(tributylstannyl) compounds.[21]

Three-bonds coupling constants $^3J(^{119}Sn, X)$ are influenced by the kind of atoms in the bonding path and possibly by the substituent groups bound to them. This effect has been recently investigated by Quintard and co-workers for $^3J(^{119}Sn\text{-}C\text{-}Z\text{-}^{13}C)$ (Z = N, O) in a series of substituted *cis*- and *trans*-2-stannyloxazolidines.[22] Some additional examples of "through N" vicinal $^{119}Sn\text{-}^{13}C$ coupling constants have been also reported for isoquinuclidine derivatives.[23]

Although the above mentioned relationships involving $^nJ(^{119}Sn, X)$ are undoubtedly useful in organotin(IV) structural studies, their use is often confined to specific structural patterns since they arise from empirical approaches. For example, in the case of di- and tri-methyltin(IV) derivatives the well-known $^2J(^{119}Sn,^1H)$ vs. θ Lockhart-Manders relationship[12] fails for *cis*-methyl configuration in hexacoordinate dimethyltin(IV) derivatives and it needs to be differently parameterized when heavy atoms, like chlorine or bromine, are bound to tin. On the other hand, as previously mentioned, Karplus-type equations for $^3J(^{119}Sn,X)$ are expected to be significantly dependent on the coupling path (i.e. the type of atoms in the path and the presence of multiple paths connecting the coupled nuclei) and on the presence of lateral substituents. In addition to this, their derivation may sometimes be hampered by the lack of experimental data for rigid systems encompassing the whole range of dihedral angles.

As far as the calculation of ^{119}Sn NMR parameters is concerned, DFT approaches have proven to be a useful methodology to support and/or predict experimental data. Chemical shifts can be accurately predicted even at the non-relativistic level due to error compensation in the calculated shielding constants,[24–28] provided no other heavy atoms are bound to tin.[29,30] Regarding the calculation of the coupling constants it has been shown that even for moderately heavy nuclei scalar relativistic effects are not negligible.[31,32] In this context relativistic ZORA DFT calculation of $^nJ(^{119}Sn,X)$ (n = 1,2; X = ^1H, ^{13}C) have been reported[29,33,34] but fully satisfactory results have not been obtained so far. For example, relativistic DFT calculations at the scalar and spin-orbit level, within the ZORA formalism, underestimated $^1J(^{119}Sn,^{13}C)$ and $^2J(^{119}Sn,^1H)$ by about a factor of 3.[29] In contrast, recent calculations at the non-relativistic DFT level of $^1J(^{119}Sn, ^{13}C)$ and $^2J(^{119}Sn, ^1H)$ of di- and trimethyltin(IV) derivatives[35] allowed to correlate these couplings with the θ angle of the dimethyltin(IV) moiety even in those cases where the aforementioned Lockhart–Manders equations fail.[12] Again, a systematic error compensation might be at the root of the observed good agreement.

In this work we present a DFT study, both at the ZORA relativistic and non-relativistic level, concerning the calculation of the $^3J(^{119}Sn,^{13}C/^1H)$ coupling constants for a series of R_3Sn^{IV} (R = Me, Bu) derivatives. The aim of the work is twofold: *i*) the validation of the computational protocols and the assessment of the importance of relativistic effects (scalar and spin-orbit) in calculating three-bonds couplings between tin and carbon or proton; *ii*) the use of the computational protocols to study in detail the dependence of the vicinal coupling constants on the dihedral angle as well as the effect of lateral substituents and multiple paths.

Results and Discussion

Comparison with Experimental Data

The molecules investigated are shown in Scheme 1. Compounds **1**–**7** have been studied experimentally by Kitching and co-workers[15] who measured the magnitude of several $^3J(^{119}Sn,^{13}C)$ in the whole range of dihedral angles, although the latter were determined using simple molecular models. They represent a very suitable set of compounds to validate our computational protocols because of their perfectly rigid structure, based on norbornyl (**1**, **2**, **6**, **7**) adamantyl (**3**, **4**) and nortricyclyl (**5**) carbon skeletons. The rotation of the trimethyltin group is not relevant to our study since all three rotamers are equivalent. The authors proposed a Karplus-type Equation (1) as

$$^3J(^{119}Sn,^{13}C) = 30.4 - 7.6\cos\phi + 25.2\cos 2\phi \quad (1)$$

for the dependence of $^3J(^{119}Sn,^{13}C)$ on the dihedral angle.

Compounds **8** and **9** have been recently studied by Santiago et al.[23] who reported some additional $^3J(^{119}Sn,^{13}C)$ coupling constants, in which, in some cases, the connection is through the nitrogen atom; although the isoquinuclidine skeleton of these molecules is rigid, there is the possibility of a *cis*/*trans* isomerism for the carbonyl group in **8** and a *syn*/*anti* isomerism for the *N*-methyl group in **9**. In addition, the butyl chains may have several *gauche*/*trans* conformations, although the investigated models are always in the all-*trans* arrangement. Some other systems based on the more flexible cyclohexane skeleton (**10**–**13**) have also been included.[17]

Finally, compounds **14**–**21** were considered by Quintard and co-workers[18] for the determination of $^3J(^{119}Sn,^2H)$ coupling constants; we note that, also in this case, only the magnitude of the coupling constants could be determined. The Karplus-type Equation (2) proposed was

$$^3J(^{119}Sn,^2H) = 8.5 - 3.0\cos\phi + 9.0\cos 2\phi \quad (2)$$

The original work was concerned with tin-deuterium coupling constants; however, if vibrational effects are neglected, they differ from tin-proton coupling constants only

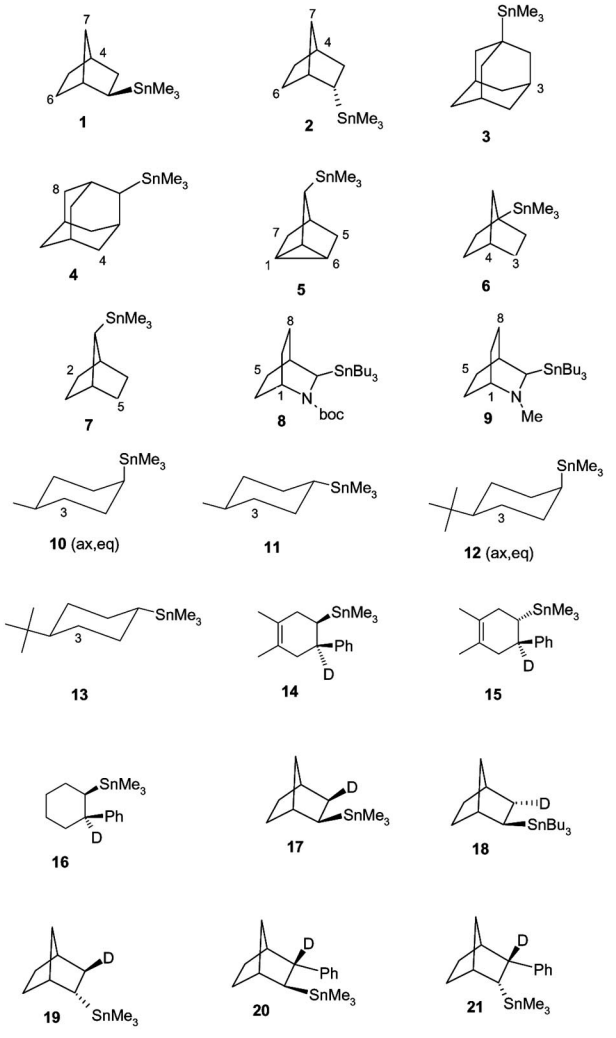

Scheme 1. Compounds investigated (boc = *tert*-butoxycarbonyl).

Table 1. Calculated and experimental $^3J(^{119}Sn,^{13}C)$ and $^3J(^{119}Sn,^1H)$ coupling constants [Hz].

Compound	^3J(SnCYX)	NON-REL[a]	REL[b]	Exp.[c]
1	SnCCC4	–9.5	–11.3	12.7
	SnCCC6	–48.7	–69.5	67.4
	SnCCC7	–0.9	2.6	0.0
2	SnCCC4	–17.4	–22.2	23.4
	SnCCC6	–28.3	–38.1	36
	SnCCC7	–44.1	–60.5	56.6
3	SnCCC3	–34.8	–49.1	51.1
4	SnCCC8	–42.7	–61.0	60.0
	SnCCC4	–6.7	–7.3	8.5
5	SnCCC1	–41.4	–51.1	53.6
	SnCCC5	–7.1	–5.2	9.7
	SnCCC6	–6.0	–5.6	8.0
	SnCCC7	–41.8	–52.8	57.8
6	SnCCC3	–38.2	–50.5	51.9
	SnCCC4	–50.7	–65.4	65.8
7	SnCCC2	–49.6	–66.2	67.5
	SnCCC5	–8.1	–9.2	11.9
8[d]	SnCNC1	–0.3	2.85	11.8
	SnCCC5	–37.7	–50.9	52.7
	SnCCC8	–13.7	–16.5	14.8
9[e]	SnCNC1	–23.3	–35.2	30.5
	SnCCC5	–46.7	–65.5	62.5
	SnCCC8	–9.9	–9.7	12.0
	SnCNMe	–4.7	–1.5	5.8
10[f]	SnCCC3	–21.8	–22.9	23.1
11	SnCCC3	–48.3	–68.8	67.5
12[g]	SnCCC3	–8.5	–8.4	12.0
13	SnCCC3	–48.1	–68.99	67.1
14	SnCCH	–110.0	–170.3	120.6
15	SnCCH	–12.9	–19.2	14.0
16	SnCCH	–104.1	–164.1	138.8
17	SnCCH	–81.0	–129.6	109.4
18	SnCCH	–25.8	–40.4	35.2
19	SnCCH	–27.3	–42.5	38.4
20	SnCCH	–73.6	–126.6	101.6
21	SnCCH	–50.4	–53.6	61.9

[a] Non-relativistic BLYP. [b] Relativistic: Scalar ZORA BLYP. [c] See text for references of the experimental values. $^3J(^{119}Sn,^2H)$ couplings have been rescaled by 6.5144 to obtain the corresponding $^3J(^{119}Sn,^1H)$ couplings. [d] Average, see text. [e] *anti* isomer. [f] Average 3:1 of (ax,eq) and (eq,ax) conformers, see ref.[17] [g] (ax,eq) conformer only, see ref.[17]

by a scaling factor given by the ratio of proton and deuterium magnetogyric ratios, that amounts to 6.5144. Therefore, in the rest of this work only coupling constants involving protons will be considered and the above Karplus-type equation will be scaled accordingly.

The calculated coupling constants, reported in Table 1, have mostly a negative sign. However there are few exceptions: ^3J(Sn-C-C-C7) in **1** and ^3J(Sn-C-N-C1) in **8** are calculated to be +2.6 Hz and +2.9 Hz, respectively, at the relativistic level, although the latter value is quite in error, see below. Notably, the dihedral angle in **1** is almost perpendicular: 93.1°. This result might have some implications because the fitting Karplus equations are obtained assuming that the coupling constants have the same sign over the entire range of the dihedral angle. However, in this particular case, the magnitude of the coupling constant with positive sign is rather small.

The correlations between experimental and calculated results are shown in Figure 1 for the whole set of data and for the $^3J(^{119}Sn,^{13}C)$ and $^3J(^{119}Sn,^1H)$, respectively. Statistical parameters are reported in Table 2. The negative slope in Figure 1 is due to the fact that the calculated, negative, ^3J coupling constant is correlated with the absolute value of the experimental one. In fact, whereas the sign of ^3J for the investigated structures is often negative,[36] there is a lack of data for some of them.

Considering the overall correlation (Figure 1 top and first two columns of Table 2), we note a very high correlation coefficient for both protocols, and, generally, a closer agreement with the calculated values of the relativistic protocol, see the lower MAE. However the slopes of the fitting lines are either higher or lower than unity. A clearer picture is obtained by looking at the $^3J(^{119}Sn,^{13}C)$ and $^3J(^{119}Sn,^1H)$ couplings in turn. For the $^3J(^{119}Sn,^{13}C)$ the performance of the relativistic protocol is very high. The statistical parameters reported in Table 2 indicate a very good correlation with an average mean absolute error (MAE) of 2.55 Hz for couplings spanning a range of about 70 Hz. It appears that

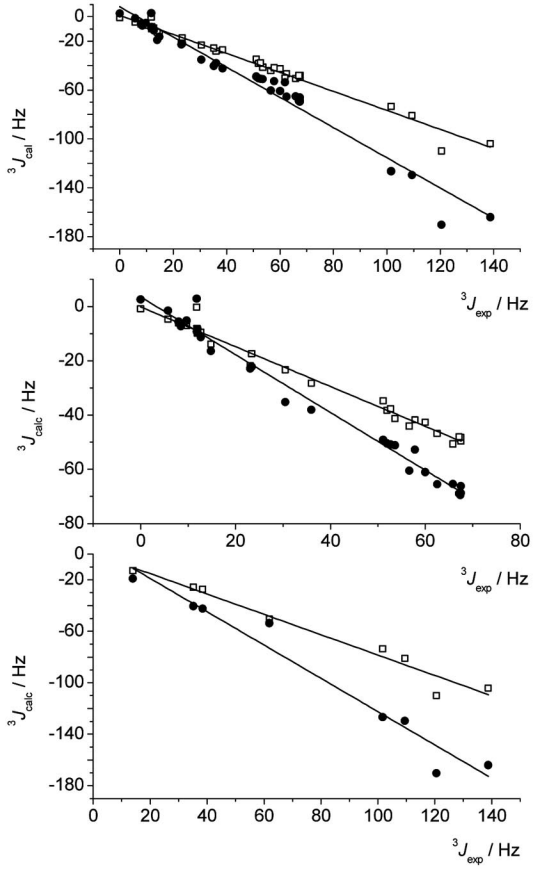

Figure 1. Correlation between calculated and experimental ^3J(Sn,X), data from Table 1. (open squares) non-relativistic level BLYP; (solid circles) relativistic level Scalar ZORA BLYP. (top panel) X = ^{1}H, ^{13}C; (middle panel) X = ^{13}C; (bottom panel) X = ^{1}H. Statistical parameters are in Table 2.

Table 2. Statistical parameters of the correlations reported in Figure 1. Mean Absolute Error, MAE = $\Sigma_i||J_{i,calc}| - |J_{i,exp}||/n$, Maximum absolute Error (ME), linear fit $J_{calc} = aJ_{exp} + b$, correlation coefficient, R^2.

	^3J(SnCYX)[a]		^3J(SnCYC)[a]	
	NON-REL	REL	NON-REL	REL
MAE (Hz)	11.08	5.95	9.44	2.55
ME(Hz)	34.66	49.74	19.20	8.95
a	–0.7767	–1.2351	–0.7332	–1.0646
b (Hz)	0.9755	8.0175	–0.1685	3.5210
R^2	0.9786	0.9666	0.9836	0.9836
	^3J(SnCCC)		^3J(SnCCH)	
	NON-REL	REL	NON-REL	REL
MAE (Hz)	9.78	2.14	16.84	17.86
ME (Hz)	19.20	5.00	34.66	49.74
a	–0.7188	–1.0438	–0.7918	–1.2950
b (Hz)	–1.0187	2.4546	0.7105	7.0564
R^2	0.9916	0.9932	0.9588	0.9548

[a] Y = N,C; X = ^{13}C,^{1}H.

only ^3J(Sn-C-N-C1) in **8** is quite in error. The calculated value is the average (as for all data of **8**) of the results obtained for the two conformers (full data are reported in Supporting Information, Tables S10 and S11). The presence of a conformational equilibrium and the difficulty in correctly modelling the flexibility of the molecule might, in part, explain the poor result obtained for this coupling constant. If this point and the few others having a nitrogen atom in the path are excluded from the statistical analysis, the performance for $^3J(^{119}Sn,^{13}C)$ becomes excellent. We also note that the results obtained for the *syn*/*anti* isomers of **9** are quite different, particularly for the ^3J(Sn,Me), see Table S12. In fact the dihedral angle Sn–C–N–Me for the optimized geometries is 27.5° and 84.4° for the *syn* and *anti* conformers, respectively. The latter structure is favoured by 2.6 kcal/mol (relativistic level) because of steric interactions in the *syn* conformer and, in fact, is the one for which calculated values are in very good agreement with the experimental results.

Vicinal couplings with protons seem, instead, less accurately reproduced with both protocols. Correlation coefficients are lower and the slopes of the fitting lines show a large deviation from unity. In particular, a very large error is found for $^3J(^{119}Sn,^1H)$ in **14** (ca. 50 Hz at the relativistic level), which markedly deviates from the linear correlation. It should be noted, however, that the calculated result only regards the conformer having a dihedral angle of approximately 180° (ax,eq), but the existence of a second conformer, with a dihedral angle of about 60° (eq,ax) cannot be ruled out (see structures (e) and (f) in Figure S1 of Supporting Information). In fact, the calculation of the coupling constant for this latter conformer provides, as expected, a significantly lower value of –18.7 Hz (see Supporting Information, Table S19). Calculations at the relativistic level predict that conformer (ax,eq) is 0.4 kcal/mol more stable than (eq,ax). Averaging the calculated *J* values by using the Boltzmann distribution at 300 K, gives a $^3J(^{119}Sn,^1H)$ of –119.1 Hz. Actually, such a good agreement with the experimental value could be fortuitous because the DFT protocol probably does not have the accuracy necessary to quantitatively describe the population of two conformers so close in energy. Nevertheless, considering the presence of a second conformer in solution certainly improves the agreement between the calculated and the experimental value. In contrast, results for compounds **15** and **16** lie on the same correlation line of the remaining values of $^3J(^{119}Sn,^1H)$: in these cases the two conformers, exchanging equatorial and axial positions, differ in energy by about 4.5 and 2.0 kcal/mol, respectively, the (eq,eq) conformer being more stable for **15** and that with axial trimethyltin being more stable for **16**. In fact the results for these latter conformers are in much better agreement with experiments than the corresponding values obtained for the other two conformers, see Tables S20 and S21.

The correlation obtained at the non-relativistic level is also very good, being the correlation coefficients essentially the same as for the relativistic protocol (see Figure 1 and Table S2 for the statistical coefficients). However there is a systematic underestimation of the magnitude of the coupling constant. This results in a slope of the fitting line, considering e.g. $^3J(^{119}Sn,^{13}C)$ couplings, of about 0.7 and, correspondingly, a larger value of the MAE. Nevertheless,

the predictive power of the non-relativistic protocol, which is computationally less expensive, is rather high once the above scaling factor is taken into account.

In contrast to the results obtained with the non-relativistic approach for ^1J and ^2J couplings, which showed a marked dependence on the functional used,[35] the results obtained for ^3J are almost independent on the particular functional and pure and hybrid ones seem to perform similarly, see Figure 2 and Table S1.

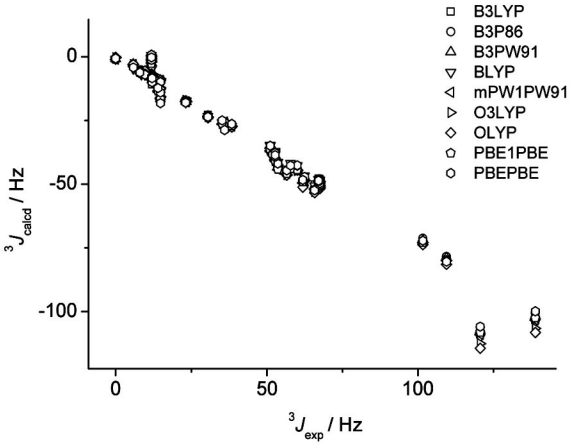

Figure 2. Correlation between calculated and experimental ^3J(Sn,X) (Hz), using several functionals at the non-relativistic level.

Finally, regarding compound **14** discussed above, it seems that the non relativistic DFT approach cannot discriminate which conformer, between (ax,eq) and (eq,ax), is the most stable. In fact, the B3LYP functional used for geometry optimization predicts that the (eq,ax) conformer is slightly more stable (by 0.05 kcal/mol), in contrast to the relativistic result. On the other hand, if the relativistic energy difference is used, the averaged $^3J(^{119}Sn,^1H)$ is –77.4 Hz, now in line with the other non-relativistic results. Thus, care should be paid when average properties are inferred from a Boltzmann population based on very small energy differences obtained from the non-relativistic approach used here.

Theoretical Karplus-Type Curves

As we have seen in the previous Section, the relativistic protocol, particularly if referred to the case of $^3J(^{119}Sn\text{-}C\text{-}C\text{-}^{13}C)$ couplings, is very accurate. With a MAE of just above 2 Hz its predictive power appears more than adequate for a detailed computational investigation of substituents, on both tin and carbon, and structural effects on the coupling constants. We have selected simple model systems, as shown in Scheme 2, and we have calculated the tin-carbon coupling constants as a function of the dihedral angle ϕ.

The effect of trimethyl, tributyl and triphenyl substituents on the tin atom has been considered, while for the γ-carbon we have considered a methyl, an isopropyl and a terbutyl group. In Figure 3 we show the results obtained for the trimethyltin(IV) model systems.

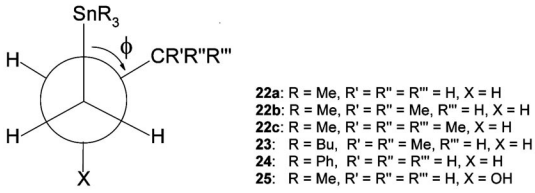

Scheme 2. Schematic representation of the model systems investigated.

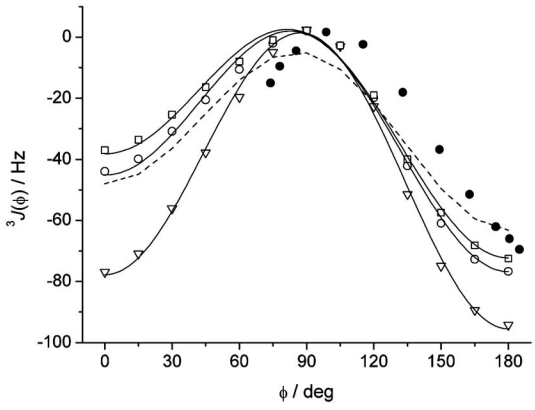

Figure 3. Calculated $^3J(^{119}Sn,^{13}C)$. (open triangles) **22a**; (open circles) **22b**; (open squares) **22c**; (solid lines): fitting curves $^3J(\phi) = A + B\cos(\phi) + C\cos(2\phi)$, parameters are reported in Table 3. (dashed line) original Karplus–Kitching curve, Equation (1).[15] (solid circles) (trimethylstannyl)cyclohexane.

The calculated coupling constants have a negative sign except in the region around 90° where they have a positive value, although rather small. Nevertheless, as already mentioned, this change of sign is of importance since all Karplus-type equations have been determined only from the magnitude of the coupling constants. If these were negative over the whole range of dihedral angles then it would suffice to change the signs of the three coefficients *A*, *B* and *C* (Table 3). On the other hand, if a change of sign occurs and the experimental data are reported only in magnitude an error in the derivation of the Karplus equations might arise.

Table 3. Fitting parameters of the Karplus-type curves of the model systems investigated for the trimethyltin(IV) model systems.

	22a ^3J(Sn,C)	**22b** ^3J(Sn,C)	**22c** ^3J(Sn,C)	**22a** ^3J(Sn,H)
A	–42.77	–30.02	–27.03	–78.17
B	8.87	15.80	17.04	29.18
C	–43.88	–30.95	–28.23	–79.64
$^3J(0°)$	–77.78	–45.17	–38.22	–128.63
$^3J(180°)$	–95.52	–76.77	–72.33	–186.99

The substitution of the hydrogen atoms of the terminal methyl group with one or more methyl groups leads to a regular decrease of the magnitude of the coupling constant except in the region around 90°, where the constant is, however, small. It is noteworthy that the Karplus–Kitching curve, also shown in Figure 3, was derived from a set of data where the vicinal carbon coupled to tin was either a

methylene or a methine group (compounds **1**–**7**). In fact, the theoretical curve obtained for the substituted model systems is rather close to the original one of Equation (1).

By fitting the calculated coupling constants with a Karplus-type curve like $^3J = A + B\cos(\phi) + C\cos(2\phi)$ we obtain the fitting coefficients reported in Table 3.

There is still some disagreement between the theoretical Karplus curves and those derived by Kitching and coworkers[15] for compounds **1**–**7**, see Equation (1). We have, therefore, investigated more in detail if this might be due to the fact that the original curve was derived for cyclic compounds where multiple coupling paths may occur. Then we have considered a model of **3** where some of the connections have been removed, as in Scheme 3.

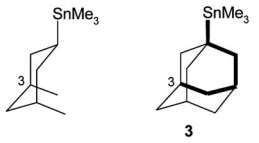

3

Scheme 3. Left: model system of **3** where one of the paths connecting Sn and C3 has been removed. Right: the original structure with the removed path highlighted.

For this model the coupling constant is now –76.7 Hz, against the calculated value for **3** of –49.1 Hz (which is in very good agreement with the experimental value of 51.1 Hz, see Table 1). This confirms that the presence of multiple paths connecting the coupled nuclei is of great importance: the magnitude of $^3J(^{119}Sn,^{13}C)$ decreases significantly by increasing the number of connections between tin and carbon; it is to note, then, that the Karplus curve derived from the polycyclic compounds **1**–**7** of Scheme 1 should be considered not strictly valid for the general case. We also emphasize that the coupling paths considered are non-equivalent and might have different signs. However, because of the complicated dependence of such couplings on the relative orientation of the bonds it is difficult to predict whether the coupling should increase or decrease for the general case.

We further investigated the multiple paths issue by deriving the Karplus-type equation for the case of (trimethylstannyl)cyclohexane by regularly varying the conformation from one chair to the other, meaning exchanging the equatorial positions to axial ones and vice versa. The Sn–C–C–C dihedral angle varies in this case from 74° to 180°. The curve is shown in Figure 3: remarkably, the maximum of the coupling is obtained for a dihedral angle of about 103° rather than 90°, as usually found. Apart from this phase shift, the curve would be rather close to that of **22b** and **22c**; however, the net result is that, for the same dihedral angle, the calculated coupling for the cyclohexane derivative is lower, in magnitude, than that obtained for a linear alkyl chain, for dihedral angles larger than about 100°; the opposite is true for smaller angles. This is in agreement with the behaviour of **3** and its model compound discussed above.

As far as the effect of the substituents on tin is concerned, see models **23** and **24** in Scheme 2, the presence of the butyl chains reduces the tin–carbon coupling constant by about 15%, as noted experimentally:[22,37] for example $^3J(0°)$ is reduced (in magnitude) from –44.0 Hz in **22b** to –38.7 in the analogous tributyl derivative **23**. Similarly, the $^3J(180°)$ is reduced from –76.7 Hz to –65.3, respectively. In contrast the presence of phenyl groups appears less clear: whereas the value of $^3J(0°)$ in **22a** is –77.0 Hz and is reduced to –74.5 Hz in **24**, $^3J(180°)$ in the same two compounds is –94.2 and –99.2 Hz, respectively, thus increasing in magnitude as methyl groups are replaced by phenyl ones; the overall effect is, however, rather small. In all cases the value of the coupling for a dihedral angle of 90° is close to zero.

Finally, we have considered the effect of an electronegative substituent bound to one of the carbon atoms on the bonding path, that is 2-hydroxy-1-(trimethylstannyl)propane, **25**, to investigate whether a substituent not directly bound to either of the coupled nuclei might have a significant influence on the coupling constants. In fact, $^3J(0°)$ is reduced from –77.0 Hz in **22a** to –56.4 Hz in **25** while $^3J(180°)$ changes from –94.2 Hz to –68.5 Hz, respectively. Therefore, there is a remarkable effect on the coupling constant even from substituents located somewhat far from the coupled nuclei.

Thus, the values of $^3J(^{119}Sn,^{13}C)$, particularly for dihedral angles of 0° or 180° where it has the largest magnitude, is a very sensitive probe of the overall structure of the molecule, carrying information not only on the relative orientation of the three bonds involved but also on the presence of substituents on or near the coupled nuclei.

Concerning the theoretical Karplus curves involving tin and proton we have calculated the coupling constants in **22a**. Results are reported in Figure 4 and in Table 3. Similarly to the $^3J(^{119}Sn,^{13}C)$ couplings, the calculated values are generally larger, in magnitude, than those predicted by the Karplus-type curve derived by Quintard and coworkers, see Equation (2). Substituent effects are expected

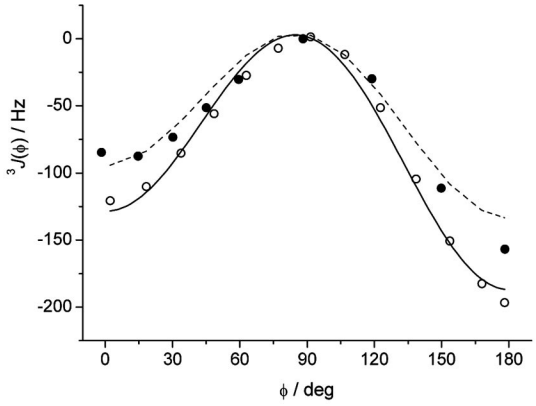

Figure 4. Calculated and experimental $^3J(^{119}Sn,^{1}H)$. Open circles: 1-(trimethylstannyl)propane, **22a**; solid line: fitting curves $^3J(\phi) = A + B\cos(\phi) + C\cos(2\phi)$, parameters are reported in Table 3; dashed line: original Karplus–Quintard curve, Equation (2);[18] solid circles: 2-hydroxy-1-(trimethylstannyl)propane (**25**).

to play a non-negligible role. We note, however, that some disagreement is also observed in the direct comparison of calculated and experimental data of $^3J(^{119}Sn,^1H)$ in compounds **14**–**21** that might be partly ascribed to conformational effects.

In Figure 4 we also compare the calculated values for **22a** with those obtained for 1-(trimethylstannyl)-2-hydroxypropane. Again, the effect of the electronegative atom is quite large, e.g. the magnitude of $^3J(180°)$ decreases from –187.0 to –156.9 Hz. Curiously, the calculated values for the hydroxy derivative almost perfectly lie on the original Karplus-type curve of Equation (2).

Conclusions

The Karplus-type dependence proposed in the literature for vicinal $^3J(^{119}Sn,^{13}C)$ and $^3J(^{119}Sn,^1H)$ coupling constants in organotin(IV) derivatives,[15,18] has been confirmed by DFT calculations for simple model systems. Scalar ZORA relativistic and non-relativistic protocols have been tested and a very good correlation with experimental values has been observed. Concerning $^3J(^{119}Sn,^{13}C)$ the relativistic protocol gives results in excellent agreement with the experimental coupling constants. On the other hand, non-relativistic protocols, computationally less expensive, have been found to perform rather well, the quality of the correlation being similar to the relativistic level; however, because of a general underestimation of the magnitude of the couplings a scaling factor is necessary if predictions have to be made. Analogous trends for the relativistic and the non-relativistic protocols have been observed for $^3J(^{119}Sn,^1H)$ although in this case the overall performance of both methods was comparable, either underestimating (non-relativistic) or overestimating (relativistic) the magnitude of the coupling constants.

Calculations showed that $^3J(^{119}Sn,^{13}C)$ and $^3J(^{119}Sn,^1H)$ couplings do not keep the same sign over the whole range of the dihedral angle: in fact, they are mostly negative except around 90°. The magnitude is, however, small in that region, so that the sign inversion does not introduce significant errors in the derivation of the Karplus equation from the experimental data, which are generally known only in absolute value.

We have also investigated the effect of substituents and molecular structure on the vicinal couplings. It has been confirmed that several factors, often overlooked, greatly affect the value of the coupling constant, namely: substituents on tin, substituents on the γ carbon and on the carbon atoms on the path as well as the presence of multiple paths connecting the coupled nuclei. Each of these contributions should be kept in mind when a Karplus-type equation is applied to the system of interest; thus, it is not possible to propose a single, general relationship valid for all the classes of vicinal coupling constants here investigated. We note, however, that the shape of the curve is not significantly altered, with the largest magnitude occurring for dihedral angles of 0° and 180°, with $|^3J(0°)| < |^3J(180°)|$, and the coupling always close to zero in the region around 90°.

Finally, as recently reported, the presence of nuclei other than carbon in the bonding path produces even larger effects on the vicinal coupling constants.[22] These effects are currently under investigation in our laboratories.

Experimental Section

Computational Details: The relativistic protocol is based on the Zeroth Order Regular Approximation (ZORA) formalism as implemented in the software package ADF.[38] Coupling constants were calculated using the *cpl* module of the software.[39] According to our previous experience,[29] and for the sake of comparison, we have selected the BLYP[40] functional and the all-electron TZ2P basis set at the scalar relativistic level. Geometry optimization were in all cases at the scalar ZORA BLYP/TZ2P level. For partially optimized geometries the dihedral angle was fixed by the application of a restraining force to the specified dihedral while all remaining coordinates were fully relaxed. At the non-relativistic level, calculations were performed with the Gaussian 03 package.[41] We have selected several functionals, of both pure and hybrid type, similarly to our previous study on $^1J(^{119}Sn,^{13}C)$ and $^2J(^{119}Sn,^1H)$,[35] and a relatively small basis set as the double zeta valence plus polarization DZVP[42] for tin and the 6-31G** for lighter atoms; an integration grid of 99 radial shells and 302 angular points in each shell was employed. All geometries were optimized by using the B3LYP[43] functional with the above basis sets. All contributions to the coupling constants have been calculated: Fermi Contact (FC), Diamagnetic and Paramagnetic Spin Orbit (DSO and PSO) and Spin Dipole (SD), although at the relativistic level the sum of FC and SD term is obtained. At the relativistic level DSO and PSO contributions, partly cancelling each other, were found to be negligible, representing no more than about 1% of the total coupling constant. At the non-relativistic level the three terms PSO, DSO and SD were all small and partly cancelling each other while the FC contribution resulted the predominant term contributing at least for the 96% to the total coupling constant value. Moreover for small coupling constants, falling in the 0–1 Hz range, even if the FC contribution is still predominant its effect is reduced to about 88–96%. Details are reported in Supporting Information, Tables S3–S26.

Solvent effects have been neglected in the present study since all experimental data were collected in low-polar solvents, such as $CDCl_3$, CS_2 or neat liquid for compounds **1**–**7**, C_6D_6 for compounds **8**, **9** and **14**–**21** and $CDCl_3$ or CCl_4 for compounds **10**–**13**. In these cases, long range solvent effects, that might be treated by continuum models, are expected to play a minor role on *J* couplings.[44]

Additional tests were run to check the convergence of the levels of theory. At the relativistic level the all-electron QZ4P basis set and the Spin-Orbit approximation were used for compound **1**. The values obtained (see Supporting Information, Tables S3 and S22) showed that neither the use of a quadruple-ζ basis set nor the inclusion of Spin-Orbit coupling in the Hamiltonian produce a significant change in the $^3J(^{119}Sn,^{13}C)$ calculated results, while a small but non-negligible effect on $^3J(^{119}Sn,^1H)$ can be observed. At the non-relativistic level the effect of basis set was tested on compound **1** by uncontracting the basis sets and adding tight s functions for the core in the calculation of the Fermi Contact term. This is accomplished by using the keyword nmr = mixed in the Gaussian03 input; in this case a large spherical product grid (200,100,200) was used. The FC terms obtained with the smaller basis set for the three coupling constants slightly differ from the corresponding val-

ues obtained with the uncontracted basis (Table 4); we also note a change in the sign of the SnCCC7 coupling which is now in agreement with the relativistic results (see "Results and Discussion" section). Differences, however, are small and non-systematic in contrast to what we found for $^1J(^{119}Sn,^{13}C)$, where the effect of the basis set was sizeable.[35] It is noteworthy that the calculation with the tight functions requires an ultrafine integration grid, as reported above, hence a whopping increase of computational time making the calculation with the larger basis set very expensive.

Table 4. Effect on the Fermi contact contribution of $^3J(^{119}Sn,^{13}C)$ for **1** on passing from the original basis sets (bs) to the uncontracted plus tight functions basis sets (ubs+s).

^3J(SnCCC)	bs	ubs+s
SnCCC4	–9.30	–7.99
SnCCC6	–47.74	–51.75
SnCCC7	–0.79	1.23

Supporting Information (see also the footnote on the first page of this article): Tables of calculated coupling constants and cartesian coordinates for all the systems investigated.

Acknowledgments

Financial support by the University of Palermo (ORPA07SY2M) is gratefully acknowledged. Calculations were run on various Linux clusters at the Laboratorio Interdipartimentale di Chimica Computazionale (LICC), Department of Chemical Sciences of the University of Padova, the Department of Chemical Physics of the University of Palermo, the Computational Chemistry Centre of Palermo (CCCP), and the Department of Inorganic and Analytical Chemistry of the University of Palermo. We thank the Fondazione Banco di Sicilia PR 13.b/07. We thank Prof. A. Bagno (Università di Padova) for useful comments.

[1] P. J. Smith, A. P. Tupčiauskas, *Ann. Rep. NMR Spectrosc.* **1978**, *8*, 291–370.
[2] R. Hani, R. A. Geanagel, *Coord. Chem. Rev.* **1982**, *44*, 229–246.
[3] B. Wrackmeyer, *Ann. Rep. NMR Spectrosc.* **1985**, *16*, 73–186.
[4] B. Wrackmeyer, *Ann. Rep. NMR Spectrosc.* **1999**, *38*, 203–264.
[5] W. H. Manders, T. P. Lockhart, *J. Organomet. Chem.* **1985**, *297*, 143–147.
[6] T. P. Lockhart, W. H. Manders, *J. Am. Chem. Soc.* **1985**, *107*, 5863–5866.
[7] M. Nádvornik, J. Holeček, K. Handlíř, *J. Organomet. Chem.* **1984**, *275*, 43–51.
[8] J. Holeček, M. Nádvornik, K. Handlíř, A. Lyčka, *J. Organomet. Chem.* **1986**, *315*, 299–308.
[9] J. Holeček, M. Nádvornik, K. Handlíř, A. Lyčka, *J. Organomet. Chem.* **1983**, *241*,177–184.
[10] I. Wharf, *Inorg. Chim. Acta* **1989**, *159*, 41–48.
[11] A. Lyčka, J. Jirman, A. Koloničny, J. Holeček, *J. Organomet. Chem.* **1987**, *333*, 305–315.
[12] T. P. Lockhart, W. F. Manders, *Inorg. Chem.* **1986**, *25*, 892–895.
[13] T. P. Lockhart, W. F. Manders, *J. Am. Chem. Soc.* **1987**, *109*, 7015–7020.
[14] J. Holeček, A. Lyčka, *Inorg. Chim. Acta* **1986**, *118*, L15–L16.
[15] D. Doddrell, I. Burfitt, M. Kitching, M. Bullpitt, C. H. Lee, R. J. Mynott, J. L. Considine, H. G. Kuivila, R. H. Sarma, *J. Am. Chem. Soc.* **1974**, *96*, 1640–1642.
[16] W. Kitching, *Org. Magn. Reson.* **1982**, *20*, 123–124.
[17] W. Kitching, H. Olszowy, J. Waugh, *J. Org. Chem.* **1982**, *43*, 898–906.
[18] J.-P. Quintard, M. Degueil-Castaing, B. Barbe, M. Petraud, *J. Organomet. Chem.* **1982**, *234*, 41–61.
[19] T. N. Mitchell, H. J. Belt, *J. Organomet. Chem.* **1990**, *386*, 167–176.
[20] T. N. Mitchell, W. Reimann, C. Nettelbeck, *Organometallics* **1985**, *4*, 1044–1048.
[21] J.-C. Meurice, J.-G. Duboudin, M. Ratier, M. Petraud, R. Willem, M. Biesemans, *Organometallics* **1999**, *18*, 1699–1705.
[22] J.-C. Cintrat, V. Léat-Crest, J.-L. Parrain, E. Le Grognec, I. Beaudet, L. Toupet, J.-P. Quintard, *Eur. J. Org. Chem.* **2004**, 4268–4279.
[23] M. Santiago, E. Low, G. Chambournier, R. E. Gawley, *J. Org. Chem.* **2003**, *68*, 8480–8484.
[24] R. Vivas-Reyes, F. De Proft, M. Biesemans, R. Willem, P. Geerlings, *J. Phys. Chem. A* **2002**, *106*, 2753–2759.
[25] P. Avalle, R. K. Harris, R. D. Fischer, *Phys. Chem. Chem. Phys.* **2002**, *4*, 3558–3561.
[26] P. Avalle, R. K. Harris, P. B. Kardakov, P. J. Wilson, *Phys. Chem. Chem. Phys.* **2002**, *4*, 5925–5932.
[27] A. Bagno, N. Bertazzi, G. Casella, L. Pellerito, G. Saielli, I. D. Sciacca, *J. Phys. Org. Chem.* **2006**, *19*, 874–883.
[28] N. Bertazzi, G. Casella, F. Ferrante, L. Pellerito, A. Rotondo, E. Rotondo, *Dalton Trans.* **2007**, *14*, 1440–1446.
[29] A. Bagno, G. Casella, G. Saielli, *J. Chem. Theory Comput.* **2006**, *2*, 37–46.
[30] H. Kaneko, M. Hada, T. Nakajima, H. Nakatsuji, *Chem. Phys. Lett.* **1996**, *261*, 1–6.
[31] M. Kaupp, M. Bühl, V. G. Malkin, *Calculation of NMR and EPR Parameters*, Wiley-VCH, Weinheim, **2004**.
[32] D. L. Bryce, R. E. Wasylishen, J. Autschbach, T. Ziegler, *J. Am. Chem. Soc.* **2002**, *124*, 4894–4900.
[33] J. Khandogin, T. Ziegler, *J. Phys. Chem. A* **2000**, *104*, 113–120.
[34] C. I. Oprea, Z. Rinkevicius, O. Vahtras, H. Ågren, K. Ruud, *J. Chem. Phys.* **2005**, *123*, 014101–014111.
[35] G. Casella, F. Ferrante, G. Saielli, *Inorg. Chem.* **2008**, *47*, 4796–4807.
[36] M. Gielen, R. Willem, B. Wrackmeyer, *Advanced Applications of NMR to Organometallic Chemistry*, Wiley, Chichester, U. K., **1996**.
[37] T. N. Mitchell, J. C. Podesta, A. Ayala, A. B. Chopa, *Magn. Reson. Chem.* **1988**, *26*, 497–500.
[38] G. de Velde, F. M. Bickelhaupt, E. J. Baerends, C. Fonseca Guerra, S. J. A. van Gisbergen, J. G. Snijders, T. Ziegler, *J. Comput. Chem.* **2001**, *22*, 931–967. http://www.scm.com.
[39] a) J. Autschbach, T. Ziegler, *J. Chem. Phys.* **2000**, *113*, 936–947; b) J. Autschbach, T. Ziegler, *J. Chem. Phys.* **2000**, *113*, 9410–9418.
[40] a) A. D. Becke, *Phys. Rev. A* **1988**, *38*, 3098–3100; b) C. Lee, W. Yang, R. G. Parr, *Phys. Rev. B* **1988**, *37*, 785–789; c) B. Miehlich, A. Savin, H. Stoll, H. Preuss, *Chem. Phys. Lett.* **1989**, *157*, 200–206.
[41] *Gaussian 03*, Revision D.02; M. J. Frisch, G. W. Trucks, H. B. Schlegel, G. E. Scuseria, M. A. Robb, J. R. Cheeseman, J. A. Montgomery Jr, T. Vreven, K. N. Kudin, J. C. Burant, J. M. Millam, S. S. Iyengar, J. Tomasi, V. Barone, B. Mennucci, M. Cossi, G. Scalmani, N. Rega, G. A. Petersson, H. Nakatsuji, M. Hada,M. Ehara, K. Toyota, R. Fukuda, J. Hasegawa, M. Ishida, T. Nakajima, Y. Honda, O. Kitao, H. Nakai, M. Klene, X.Li, J. E. Knox, H. P. Hratchian, J. B. Cross, V. Bakken, C. Adamo, J. Jaramillo, R. Gomperts, R. E. Stratmann, O. Yazyev, A. J. Austin, R. Cammi, C. Pomelli, J. W. Ochterski, P. Y. Ayala, K. Morokuma, G. A. Voth, P. Salvador, J. J. Dannenberg, V. G. Zakrzewski, S. Dapprich, A. D. Daniels, M. C. Strain, O. Farkas, D. K. Malick, A. D Rabuck, K. Raghavachari, J. B. Foresman, J. V. Ortiz, Q. Cui, A. G. Baboul, S. Clifford, J. Cioslowski, B. B. Stefanov, G. Liu, A. Liashenko, P. Piskorz, I. Komaromi, R. L. Martin, D. J. Fox, T. Keith, M. A. Al-Laham, C. Y. Peng, A. Nanayakkara, M. Challacombe, P. M. W. Gill, B. Johnson, W. Chen, M. W. Wong, C. Gonzalez, J. A. Pople, *Gaussian*, Inc., Wallingford CT, **2004**.

[42] a) N. Godbout, D. R. Salahub, J. Andzelm, E. Wimmer, *Can. J. Chem.* **1992**, *70*, 560–571; b) K. L. Schuchardt, B. T. Didier, T. Elsethagen, L. Sun, V. Gurumoorthi, J. Chase, J. Li, T. L. Windus, *J. Chem. Inf. Model.* **2007**, 1045–1052.
[43] a) P. J. Stephens, F. J. Devlin, C. F. Chabalowski, M. J. Frisch, *J. Phys. Chem.* **1994**, *98*, 11623–11627; b) R. H. Hertwig, W. Koch, *Chem. Phys. Lett.* **1997**, *268*, 345–351.
[44] A. Bagno, F. Rastrelli, G. Saielli, *Prog. NMR Spectrosc.* **2005**, *47*, 41–93.

Received: February 25, 2009
Published Online: June 3, 2009

